Nanocrack-induced leakage current in AlInN/AlN/GaN

Albert Minj Daniela Cavalcoli Saurabh Pandey Beatrice Fraboni
Anna Cavallini Tommaso Brazzini and Fernando Calle

Here we report on the study of nano-crack formation in $Al_{1-x}In_xN$/AlN/GaN heterostructures, on its association with composition fluctuation and on its local electrical properties. It is shown here that indium segregation at nano-cracks and threading dislocations originating from the non-pseudomorphic AlN interlayer could be the cause of the high reverse-bias gate leakage current of Ni/Au Schottky contacts on $Al_{1-x}In_xN$/AlN/GaN heterostructures and significantly affects the contact rectifying behavior. Segregation of indium around crack tips in $Al_{1-x}In_xN$ acting as conductive paths was assessed with conductive atomic force microscopy.

Keywords: C-AFM; Indium; Segregation; Nano-cracks; AlInN/AlN/GaN

AlGaN/GaN heterostructures are widely used in high electron mobility transistor (HEMT) devices due to the presence of strong spontaneous and piezoelectric polarization fields that cause the formation of high two-dimensional electron gas (2DEG) density ($\sim 1 \times 10^{13}$ cm^{-2}) [1]. However, AlGaN/GaN heterostructures are strongly lattice-mismatched, especially at high Al content. Recently, lattice-matched AlInN/GaN heterostructures have been investigated in view of their potential application to HEMT devices [2]. In AlInN/GaN the strong spontaneous polarization field induces a 2DEG electron density reaching up to 2.4×10^{13} cm^{-2} [2]. Nevertheless, the alloy-disorder effect in the AlInN barrier layer prevents such structure from achieving a high mobility in the channel. In order to reduce alloy-disorder effect, the insertion of an AlN layer between AlInN and GaN is often used [2,3]. The idea of using AlN as an insertion layer was drawn from its use in AlGaN/GaN heterostructures, where it was introduced to grow crack-free thick AlGaN layers [4]. In that case it was found that the introduction of a relaxed AlN thin film (i.e., with thickness beyond its critical value) causes compressive strain in the AlGaN layer, thus preventing it from cracking. Moreover, crack propagation from the AlN interlayer into the AlGaN layer wasn't observed.

In lattice-matched AlInN, there is an additional advantage, as the higher conduction band offset due to presence of the AlN layer provides a better electron confinement [5]. It was shown that electron mobility and 2DEG concentration vary with the thickness of AlN layer [3,6], both increasing for higher AlN thickness. On the other hand, for an indium concentration of 13%, there would be compressive strain in the AlInN barrier when grown over a relaxed AlN layer, and crack formation is not expected in a compressively strained layer. On the contrary, we have observed crack formation and high density of V pits ($\sim 10^{10}$ cm^{-2}) in $Al_{0.87}In_{0.13}N$ barrier layers.

When AlN is grown over GaN (0001), it is under tensile strain. Its critical thickness reported for strain relaxation is ~6.5 nm [5]. It is known that beyond the critical thickness strain an AlN layer would be released non-pseudomorphically by crack formation and generation of threading dislocations (TDs). However, in the case of the sandwich structure of AlN between GaN and $Al_{0.87}In_{0.13}N$ layer as ours, cracking mechanism may take place for thickness lower than 6.5 nm because of the additional tensile strain induced by the $Al_{0.87}In_{0.13}N$ layer.

In this work, we have studied the role of relaxed AlN interlayers in AlInN/AlN/GaN heterostructures in terms of crack propagation and additional threading

dislocations into the barrier layer, together with the effect that the AlN interlayer plays on the electrical properties.

AlInN/AlN/GaN heterostructures have been grown on *c*-plane sapphire substrates in an Aixtron MOCVD reactor with varying interlayer AlN thickness as 0 (A), 0.5 nm (B), 1 nm (C), 1.5 nm (D), 2.5 nm (E) and 7.5 nm (F). Nominal thicknesses of the AlInN and GaN layers were ~15 nm and 3 μm, respectively. Indium concentration in these samples varies between 13% and 14% as assessed by high resolution X-ray diffraction (HRXRD). Surface morphology and surface inhomogeneity have been characterized using atomic force microscopy (AFM) (NT MDT-Solver PRO 47) in semi-contact mode (phase imaging). Conductivity maps at the nanoscale have been obtained using Ag_2Ga nano-needle (Nauga nano-needles) as an AFM tip [7]. The contact area formed between AFM tip and sample surface was ~5–10 nm^2. The ohmic and Schottky contacts have been prepared by evaporating Ti/Al/Ni/Au metals (annealed at 850 °C for 30 s in N_2 ambient) and Ni/Au metals (circular Schottky contacts 1 mm diameter), respectively, for current–voltage characterization. Hall measurements have been also performed on these samples [8].

AFM topography images (semi-contact mode) of samples A–E, with AlN thickness varying from 0 to 2.5 nm, indicated that the surface consists of grain-like features of average grain radius of 60 nm (see Fig. 1), which are typical of MOCVD AlInN/GaN heterostructures, with threading dislocations in the form of V defects [9]. In the samples with the narrower AlN interlayer thickness (up to 2.5 nm), the density of V defects is found to be almost constant, ~10^8 cm^{-2}, which is a typical value found on the surface of 3 μm thick GaN (0 0 0 1) layer grown over sapphire substrate [10]. In-segregation associated with V defects in AlInN/AlN/GaN structures [9,11] have been speculated to be the cause of increased leakage current in Schottky contacts [12–14] when compared to AlGaN/GaN heterostructures. In sample F, with a higher AlN thickness of ~7.5 nm, surface regions containing both a high density of cracks and V-pit/threading dislocations (density ~10^{10} cm^{-2}) have been observed. Figure 2a shows a detail of cracks imaged in sample F by semi-contact mode AFM.

We have observed that cracks are not uniformly distributed over the surface. Non-uniformity of the AlN layer thickness could be the possible reason for the observed inhomogeneous distribution of the crack density. Micro-cracks (from a few μm to a few 100 μm) have been already reported in the literature [15,16], but the nano-cracks investigated in the present work are significantly smaller in size. In our sample F, cracks are at most 150 nm long and 15–50 nm wide.

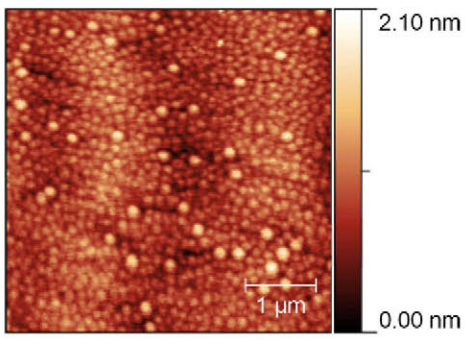

Figure 1. Topography image (semi-contact) of sample with AlN thickness = 1 nm showing absence of cracks.

Phase-contrast mode (semi-contact AFM) and C-AFM have been useful in the detection of indium segregation at TDs in our previous work [9]. During the growth of AlInN on the AlN layer with crack channels, segregation of In adatoms around the edges of crack tips is energetically favored, because low coordination sites are preferentially occupied by the weaker In–N bonds rather than by the stronger Al–N bonds [17]. This would result in the formation of an indium-rich path between the surface and the AlInN/AlN interface at the crack as the AlInN layer grows. Figure 2b is a 1 × 1 μm^2 current AFM map obtained with a bias voltage of 3.5 V on sample F, with the dark regions corresponding to higher currents. This clearly shows that the edges of the crack channels (dark contrast) are more conductive than the other regions. Figure 3a shows the topography and Figure 3b shows the phase-contrast map obtained simultaneously in semi-contact mode AFM. In the latter figure, a strong contrast occurs at the crack edges, which is related to changes in composition or strain energy [18,19]. Since migration of In adatoms is well known to be governed by strain energy [17,20], this contrast would also depict the compositional variation near the crack edges. As described above, this could be associated to In adatoms concentrating along the edges of cracks, leading to the formation of conductive paths between the surface and the 2DEG. Therefore, we can ascribe the dark contrast observed at these regions, both in phase images and in current maps, to the presence of high In content.

I–V characteristics obtained with an AFM probe at the cracks, Figure 4a, show a significant increase in the current with increasing applied bias, almost symmetric in forward bias and reverse bias. This indicates that cracks act as shunts between the surface and the 2DEG even at low voltages, hence providing a conductive electrical path. On the contrary, *I–V* at a crack-free surface shows the conduction onset in forward bias only at voltages larger than 7 V.

Figure 4b shows the comparison between room temperature *I–V* curves of Ni/Au Schottky contacts on AlInN/AlN/GaN heterostructures with AlN thickness of 7.5 nm (sample F) and of 1 nm (sample C). The leakage current density for the 7.5 nm thick AlN layers is 0.157 A cm^{-2} at a reverse bias of 2 V, which is almost one order of magnitude higher than for samples with 1 nm thick AlN layers (0.017 A cm^{-2}). It is also noteworthy that the presence of the cracked 7.5 nm thick AlN layer induces a marked degradation of the rectifying properties of the Schottky contacts ($I_{\text{Forward Bias}}/I_{\text{Reverse Bias at V = +2 V}} = 2.96$), leading to an almost ohmic behavior. This effect could be associated to the presence of electrically active nano-cracks and to a high density of V defects. These results, dealing with the macroscopic electrical behavior, correlate well with what we observed at microscopic level from *I–V* obtained with an AFM probe at the cracks, shown in Figure 4a.

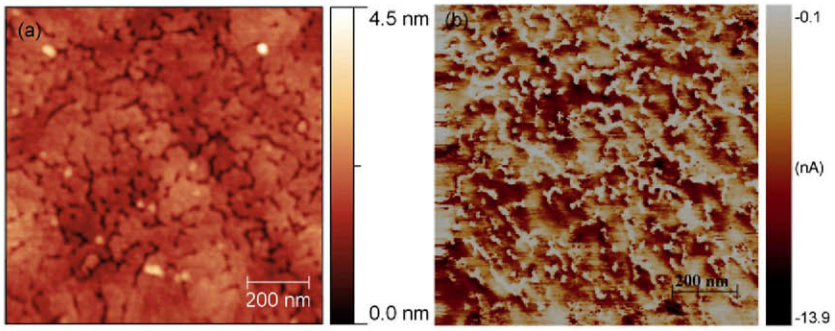

Figure 2. (a) Topography image (semi-contact) of sample F, AlN thickness = 7.5 nm showing cracks. (b) Current map of sample F. Dark-contrast regions indicate high current/In-rich regions. Current map here does not correspond to the same area shown in (b) above.

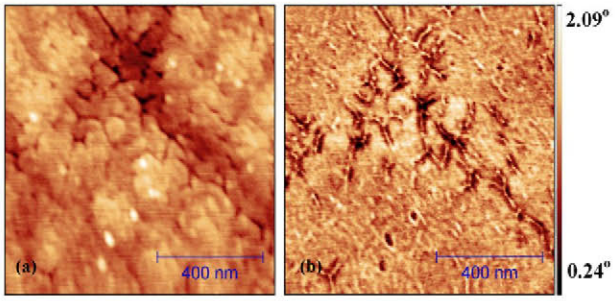

Figure 3. (a) Topography image of sample F (semi-contact mode AFM) showing cracks, and (b) corresponding phase image. Dark-contrast regions are associated to In segregation.

As reported in Ref. [8], Hall measurements demonstrate for the sample F (7.5 nm thick non-pseudomorphic AlN layer) a lower 2DEG concentration (2×10^{13} cm^{-2}) and a lower mobility (300 cm^{-2}V^{-1}s^{-1}) than those samples with a pseudomorphically grown AlN interlayer (A–E). These results in terms of 2DEG density differ from those calculated for pseudomorphic AlN with 7.0 nm or more (for thickness more than critical thickness of AlN), where high sheet carrier concentration is hypothesized [5]. To understand the effect of these structural defects formations that includes both nanocracks and threading dislocations, the non-pseudomorphic AlN layer (7.5 nm) grown over GaN can be roughly modeled as a layer with local thickness fluctuations, reducing to 0 nm as the worst case. As we know, the sheet carrier concentration is a function of the barrier height, of the band offset and of the barrier and interlayer thickness [21]. Because of the possibility of low quality of metalorganic chemical vapor deposition (OCVD)-grown AlN (as they were grown at a low temperature, 750 °C) in terms of its surface roughness, local fluctuations in thickness can be expected. But local fluctuations in AlN thickness still cannot explain the observed lowering of sheet carrier concentration because high 2DEG density was observed in all the samples with varying AlN thickness from 0 to 2.5 nm. On the other hand, the presence of high indium segregation at these defects would cause local reduction in polarization fields, in barrier height and in band gap and this would explain the observed low 2DEG electron density. In order to understand also the low mobility values, scattering mechanisms need also to be accounted for. Scattering due to structural defects (such as cracks, high density of dislocations) [22] and alloy disorder [23] due to indium segregation stand as the dominating candidates for the cause of low mobility.

In conclusion, AFM analyses carried out in semi-contact and conductive mode allowed for the identification and characterization of nano-cracks in AlInN/AlN/GaN heterostructures. We have here assessed that this propagation is associated with indium segregation. Current–voltage characteristics show that the nanocracks are electrically conductive, induce very high leakage current and strongly affect the rectifying behavior of Schottky contacts fabricated on the AlInN layer.

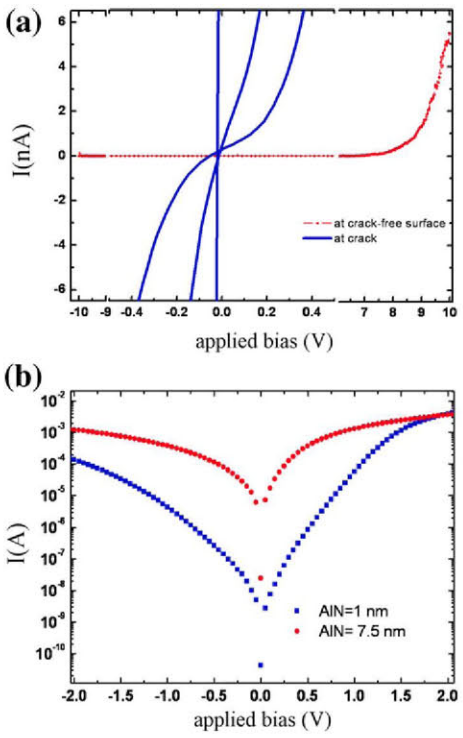

Figure 4. (a) Microscopic current–voltage characteristics obtained with the AFM-probe at the cracks and on a crack-free surface of AlInN/AlN (7.5 nm)/GaN heterostructures (sample F). (b) Macroscopic current–voltage characteristics of Ni/Au Schottky contacts on AlInN/AlN/GaN heterostructures with AlN layers of 7.5 nm (sample F) and 1 nm (sample C).

Aixtron SE, Herzogenrath, Germany and RWTH Aachen, Aachen, Germany are gratefully acknowledged for sample growth and useful discussions.

[1] O. Ambacher, B. Foutz, J. Smart, J.R. Shealy, N.G. Weimann, K. Chu, M. Murphy, A.J. Sierakowski, W.J. Schaff, L.F. Eastman, R. Dimitrov, A. Mitchell, M. Stutzmann, J. Appl. Phys. 87 (2000) 334–344.
[2] M. Gonschorek, J.–F. Carlin, E. Feltin, M.A. Py, N. Grandjean, Appl. Phys. Lett. 89 (2006) 062106.
[3] A. Teke, S. Gokden, R. Tulek, J.H. Leach, Q. Fan, J. Xie, U. Ozgur, H. Morkoc, S.B. Lisesivdin, E. Ozbay, New J. Phys. 11 (2009) 063031.
[4] C. McAleese, M.J. Kappers, F.D.G. Rayment, P. Cherns, C.J. Humphrey, J. Crys, Growth 272 (2005) 475–480.
[5] Y. Cao, Debdeep Jena, Appl. Phys. Lett. 90 (2007) 182112.
[6] J. Xie, X. Ni, M. Wu, J.H. Leach, Ü. Özgür, H. Morkoç, Appl. Phys. Lett. 91 (2007) 132116.
[7] Mehdi M. Yazdanpanah, Steven A. Harfenist, Abdelilah Safir, Robert W. Cohn, J. Appl. Phys. 98 (2005) 073510.
[8] S. Pandey, B. Fraboni, D. Cavalcoli, A. Minj, A. Cavallini, Appl. Phys. Lett. 99 (2011) 012111.
[9] A. Minj, D. Cavalcoli, A. Cavallini, Appl. Phys. Lett. 97 (2010) 132114.
[10] A. Minj, D. Cavalcoli and A. Cavallini, Phy. Stat. Solidi (in-press).
[11] Z.L. Miao, T.J. Yu, F.J. Xu, J. Song, C.C. Huang, X.Q. Wang, Z.J. Yang, G.Y. Zhang, X.P. Zhang, D.P. Yu, B. Shen, Appl. Phys. Lett. 95 (2009) 231909.
[12] E. Arslan, S. Butun, E. Ozbay, Appl. Phys. Lett. 94 (2009) 142106.
[13] E. Arslan, Ş. Altındal, S. Özçelik, E. Ozbay, Semicond. Sci. Technol. 24 (2009) 075003.
[14] W. Chikhaoui, J.-M. Bluet, M.-A. Poisson, N. Sarazin, C. Dua, C. Bru-Chevallier, Appl. Phys. Lett. 96 (2010) 072107.
[15] S.J. Hearne, J. Han, S.R. Lee, J.A. Floro, D.M. Follstaedt, E. Chason, I.S.T. Tsong, Appl. Phys. Lett. 76 (2000) 1534–1536.
[16] M.Germain, M. Leys, S. Boeykens, S. Degroote, W.Wang, D. Schreurs, W. Ruythooren, K.Choi, B. Van Daele, G. Van Tendeloo, G. Borghs, Mat. Res. Soc. Symp., Proc. 798 (2004) Y10.22.1.
[17] Th. Kehagias, G.P. Dimitrakopulos, J. Kioseoglou, H. Kirmse, C. Giesen, M. Heuken, A. Georgakilas, W. Neumann, Th. Karakostas, P. Komninou, Appl. Phys. Lett. 95 (2009) 071905.
[18] R. García, R. Magerle, R. Perez, Nat. Mater. 6 (2007) 405–411.
[19] M. Jung, J.W. Choi, Ultramicroscopy 110 (2010) 670–675.
[20] J.E. Northrupa, L.T. Romano, Appl. Phys. Lett. 74 (1999) 2319.
[21] M. Gonschorek, J-F. Carlin, E. Feltin, M. Py, N. Grandjean, Int. J. Microw. Wireless Technol. 2 (1) (2010) 13–20.
[22] D.C. Look, J.R. Sizelove, Phys. Rev. Lett. 82 (1999) 61237–61240.
[23] A. Teke, S. Gökden, R. Tülek1, J.H. Leach, Q. Fan, J. Xie, Ü. Özgür, H. Morkoç, S.B. Lisesivdin, E. Özbay, New J. Phys. 11 (2009) 063031.